Novel Roles for the Polyphenol Oxidase Enzyme in Secondary Metabolism and the Regulation of Cell Death in Walnut[1][W][OPEN]

Soha Araji, Theresa A. Grammer, Ross Gertzen, Stephen D. Anderson, Maja Mikulic-Petkovsek, Robert Veberic, My L. Phu, Anita Solar, Charles A. Leslie, Abhaya M. Dandekar, and Matthew A. Escobar*

Department of Biological Sciences, California State University, San Marcos, California 92096 (S.A., T.A.G., R.G., S.D.A., M.A.E.); Department of Agronomy, Biotechnical Faculty, University of Ljubljana, Jamnikarjeva 101, SI–1000 Ljubljana, Slovenia (M.M.-P., R.V., A.S.); and Department of Plant Sciences, University of California, Davis, California 95616 (M.L.P., C.A.L., A.M.D.)

The enzyme polyphenol oxidase (PPO) catalyzes the oxidation of phenolic compounds into highly reactive quinones. Polymerization of PPO-derived quinones causes the postharvest browning of cut or bruised fruit, but the native physiological functions of PPOs in undamaged, intact plant cells are not well understood. Walnut (*Juglans regia*) produces a rich array of phenolic compounds and possesses a single PPO enzyme, rendering it an ideal model to study PPO. We generated a series of PPO-silenced transgenic walnut lines that display less than 5% of wild-type PPO activity. Strikingly, the PPO-silenced plants developed spontaneous necrotic lesions on their leaves in the absence of pathogen challenge (i.e. a lesion mimic phenotype). To gain a clearer perspective on the potential functions of PPO and its possible connection to cell death, we compared the leaf transcriptomes and metabolomes of wild-type and PPO-silenced plants. Silencing of PPO caused major alterations in the metabolism of phenolic compounds and their derivatives (e.g. coumaric acid and catechin) and in the expression of phenylpropanoid pathway genes. Several observed metabolic changes point to a direct role for PPO in the metabolism of tyrosine and in the biosynthesis of the hydroxycoumarin esculetin in vivo. In addition, PPO-silenced plants displayed massive (9-fold) increases in the tyrosine-derived metabolite tyramine, whose exogenous application elicits cell death in walnut and several other plant species. Overall, these results suggest that PPO plays a novel and fundamental role in secondary metabolism and acts as an indirect regulator of cell death in walnut.

Polyphenol oxidases (PPOs) are a group of copper-containing enzymes that catalyze the *o*-hydroxylation of monophenols to *o*-diphenols (tyrosinase activity, Enzyme Commission 1.14.18.1) as well as the oxidation of *o*-diphenols to quinones (catecholase activity, Enzyme Commission 1.10.3.2) in the presence of oxygen. These enzymes are broadly distributed among animals, fungi, and plants, though many plant PPOs appear to lack tyrosinase activity (Steffens et al., 1994). The study of PPOs in plants has focused primarily on their role in the process of postharvest browning, whereby cut or damaged plant tissues turn brown due to the polymerization of PPO-generated quinones, generating phytomelanins (Mesquita and Queiroz, 2013). Classically, PPOs and their potential phenolic substrates have been considered to be physically separated from one another in intact plant cells, with most PPOs targeted to the chloroplasts, while phenolic compounds accumulate primarily in the vacuole and cell wall (Vaughn et al., 1988; Steffens et al., 1994). Thus, PPO activity in vivo has typically been associated with senescing, wounded, or damaged plant tissues in which cellular compartmentalization is lost (Steffens et al., 1994).

PPOs are most commonly encoded by multigene families in plants, ranging in size from 13 PPO genes in *Physcomitrella patens* to two PPO genes in rice (*Oryza sativa*). However, several plant species, including cucumber (*Cucumis sativus*), cassava (*Manihot esculenta*), and walnut (*Juglans regia*), have only a single PPO gene, and Arabidopsis (*Arabidopsis thaliana*) lacks PPO altogether (Escobar et al., 2008; Tran et al., 2012). Within a single plant species, different members of the PPO gene family can display quite divergent regulatory patterns, with expression in different tissues or in the same tissue but at different developmental stages (Thygesen et al., 1995; Thipyapong and Steffens, 1997; Kim et al., 2001). Many PPO genes have been shown to be up-regulated by wounding, pathogens, and/or stress-associated hormones such as methyl jasmonate and salicylic acid (SA), but responsiveness to these cues again varies between species and within PPO gene families (Constabel and Ryan, 1998). For example, in the five-member PPO gene family in dandelion (*Taraxacum officinale*), only *ppo2* is responsive to pathogen infection (Richter et al., 2012).

[1] This work was supported in part by a University of California/California State University Collaborative Research Grant.

* Address correspondence to mescobar@csusm.edu.

The author responsible for distribution of materials integral to the findings presented in this article in accordance with the policy described in the Instructions for Authors (www.plantphysiol.org) is: Matthew A. Escobar (mescobar@csusm.edu).

[W] The online version of this article contains Web-only data.

[OPEN] Articles can be viewed online without a subscription.

www.plantphysiol.org/cgi/doi/10.1104/pp.113.228593

Although PPO was once described as "the chloroplast oxidase with no established function" (Vaughn et al., 1988), more recent studies have shed some light on possible functions of PPOs in plants. Best characterized is a role of some PPO genes in plant defense against insects and pathogens. As previously discussed, many PPO genes are up-regulated upon pathogen challenge, and overexpression of a potato (*Solanum tuberosum*) PPO in tomato (*Solanum lycopersicum*) resulted in decreased susceptibility to *Pseudomonas syringae* pv *tomato* (Li and Steffens, 2002). Likewise, silencing of PPOs in tomato led to increased disease susceptibility (Thipyapong et al., 2004). Similarly, overexpression of PPO genes in tomato and hybrid aspen (*Populus tremula* × *Populus alba*) resulted in increased insect resistance, and silencing of PPOs resulted in increased susceptibility to insect herbivory (Wang and Constabel, 2004; Mahanil et al., 2008; Bhonwong et al., 2009). PPO also plays a central role in the polymerization of glandular trichome exudates in wild potato (*Solanum berthaultii*), a process that entraps small insects such as aphids (Kowalski et al., 1992).

PPOs have also been implicated in the biosynthesis of some specialized pigments and other secondary metabolites. Specific PPOs are required for the synthesis of aurone pigments in snapdragons (*Antirrhinum majus*) and betalin pigments in the order Caryophyllales (Nakayama et al., 2001; Gandía-Herrero et al., 2005). PPO also has a central role in the biosynthesis of 8-8′ linked lignans in creosote bush (*Larrea tridentata*; Cho et al., 2003). Given the diverse regulation and characterized functions of PPO genes, it appears likely that different PPOs within a gene family may play a variety of roles in the physiology and development of a single plant.

Walnut presents an interesting model to further explore the function(s) of PPOs in plants, in that walnuts generate an exceptionally diverse array of phenolic compounds (Colaric et al., 2005; Solar et al., 2006) and possess a single PPO gene, *jrPPO1* (Escobar et al., 2008). *JrPPO1* appears to be constitutively expressed at a high level in all green tissues and is not responsive to wounding or methyl jasmonate treatment (Escobar et al., 2008). To better understand the functional role of the single PPO enzyme in walnut, we used RNA interference (RNAi) to generate a series of transgenic walnut lines with greatly reduced PPO activity. Surprisingly, these transgenic lines displayed a lesion mimic phenotype, spontaneously developing necrotic spots on their leaves independent of pathogen infection. Results from global transcript and metabolite profiling of the PPO-silenced lines suggest that JrPPO1 plays a fundamental role in the metabolism of Tyr in vivo and that, in the absence of PPO, the toxic metabolite tyramine accumulates to high levels in walnut leaves.

RESULTS

Generation and Characterization of PPO-Silenced Walnut Lines

To manipulate the levels of active PPO enzyme in walnut and study the resulting phenotypic effects, walnut somatic embryos were transformed with two binary vectors: one designed to constitutively overexpress the *jrPPO1* gene and one designed to silence the *jrPPO1* gene. We recovered and germinated two lines transformed with the overexpression vector and nine lines transformed with the RNAi vector. Nontransformed walnut somatic embryos were germinated in parallel to provide matched wild-type controls. Following transfer to soil, we collected leaves from these transgenic plants, extracted total protein, and performed PPO enzyme activity assays, using L-3,4-dihydroxy-Phe (L-DOPA) as substrate (Fig. 1). All of the RNAi lines showed more than 95% reduction in leaf PPO activity, demonstrating highly efficient silencing of *jrPPO1*. Corresponding reductions in *jrPPO1* mRNA levels were also demonstrated via real-time reverse transcription-PCR (RT-PCR) analysis of selected RNAi lines (Supplemental Fig. S1). Surprisingly, the "overexpression" lines (40-1-1, 78-2-8) also showed large reductions in leaf PPO activity, indicating the activation of cosuppression rather than successful overexpression of *jrPPO1*.

The existence of transgenic walnut lines showing near-complete suppression of PPO activity allowed us to examine which of the diverse group of phenolic compounds generated by walnuts could potentially serve as substrates for JrPPO1. Caffeic acid, chlorogenic acid, and catechin are *o*-diphenols that are naturally synthesized in walnut leaves and/or hulls (Colaric et al., 2005; Solar et al., 2006). These phenolics were utilized as substrates in polarimetric PPO activity assays (catecholase activity), using total protein extracts from either wild-type leaves or leaves from a randomly selected PPO-silenced line (9-5-1). The PPO-silenced line served as a negative control, assuring that any observed activity (oxygen consumption) could be attributed specifically to PPO. As summarized in Figure 2A, each of these native substrates could be

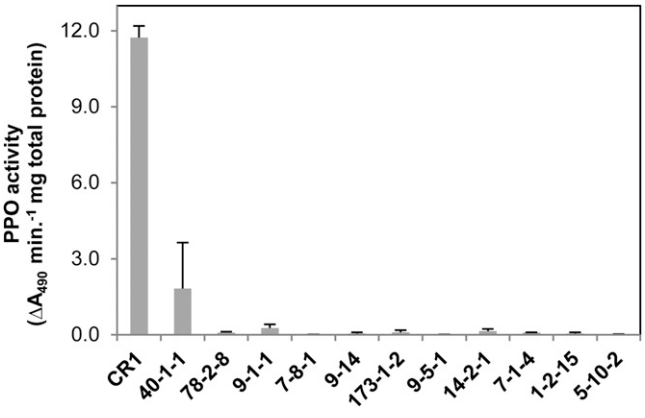

Figure 1. PPO protein activity in leaf protein extracts from wild-type walnut (CR1) and transgenic walnut lines. Lines 40-1-1 and 78-2-8 were transformed with a *jrPPO1* overexpression vector, and all other transgenic lines were transformed with a *jrPPO1* silencing vector. PPO activity was measured spectrophotometrically by monitoring dopachrome accumulation at 490 nm using L-DOPA as a substrate. For each line, the mean activity from three biological replicates (± SEM) is presented.

effectively oxidized by PPO in vitro, with no activity detected in protein extracts from the silenced line. Substrate kinetics for each of these *o*-diphenols is presented in Table I. We also examined the native monophenols Tyr, tyramine, and *p*-coumaric acid as potential substrates for JrPPO1. In general, PPOs display much lower tyrosinase activities than catecholase activities (i.e. the hydroxylation of monophenols is much slower than the oxidation of *o*-diphenols; Selinheimo et al., 2007; Goldfeder et al., 2013), and this was also true for JrPPO1 (Supplemental Fig. S2). To simplify measurement of the relatively low in vitro tyrosinase activities, PPO assays utilizing monophenol substrates were performed spectrophotometrically. As summarized in Figure 2B, all three monophenols could be utilized as substrates by JrPPO1, though activity was substantially lower for *p*-coumaric acid than for Tyr and tyramine.

Phenotyping PPO-Silenced Walnut Lines

Given previous research suggesting a role for some PPOs in plant defense (Li and Steffens, 2002), we initially planned to perform a series of pathogen challenge bioassays on the PPO-silenced walnut lines and matched wild-type controls. These plans were almost immediately abandoned, however, because shortly after transfer to soil, the PPO-silenced lines (but none of the wild-type controls) spontaneously developed scattered necrotic lesions on their leaves (Fig. 3). The development of these lesions has been observed in the PPO-silenced lines in four consecutive growing seasons, with trees grown at two separate locations (Davis, CA; San Marcos, CA). Once formed, the lesions are typically static, though they can coalesce late in the season, causing premature leaf drop (Fig. 3). We initially believed that the leaf necrosis was caused by naturally occurring pathogen infection, given that PPO-silenced tomatoes have previously been shown to be hypersusceptible to bacterial speck disease (Thipyapong et al., 2004). Two walnut diseases can generate scattered leaf necrosis symptoms: walnut blight (causal agent, *Xanthomonas arboricola* pv *juglandis*) and walnut anthracnose (causal agent, *Gnomonia leptostyla*; Cline and Neely, 1983; Belisario et al., 1999). Attempts to isolate *X. arboricola* pv *juglandis* from the necrotic lesions on PPO-silenced lines were unsuccessful, though the pathogen could be readily isolated from artificially inoculated wild-type plants (data not shown; Belisario et al., 1999). The lesions also lacked the small fruiting bodies (acervuli) that are diagnostic features of walnut anthracnose, and attempts to isolate *G. leptostyla* mycelia from leaf discs containing necrotic tissue were also unsuccessful (Belisario et al., 2008). In addition, the lesions were completely static when detached leaves were incubated in a moist chamber, with no formation of fungal fruiting bodies, bacterial ooze, or increase in lesion size. Thus, the necrotic spots that form on the leaves of PPO-silenced walnut plants appear to be independent of pathogen challenge and were thus classified as a lesion mimic phenotype.

Previous studies of lesion mimic mutants, which are defined by their inappropriate activation of programmed cell death, identified alterations in SA and/or reactive oxygen species metabolism as potential underlying components (Lorrain et al., 2003). Thus, we compared the relative levels of SA, H_2O_2, and malondialdehyde (a lipid peroxidation product used as an indicator of oxidative damage) in PPO-silenced leaves and wild-type leaves. However, no significant differences in SA, H_2O_2, or oxidative damage were detected between the lines (Supplemental Figs. S3–S5). Thus, the mechanistic connection between PPO and the lesion mimic phenotype would appear to operate via a previously undescribed pathway.

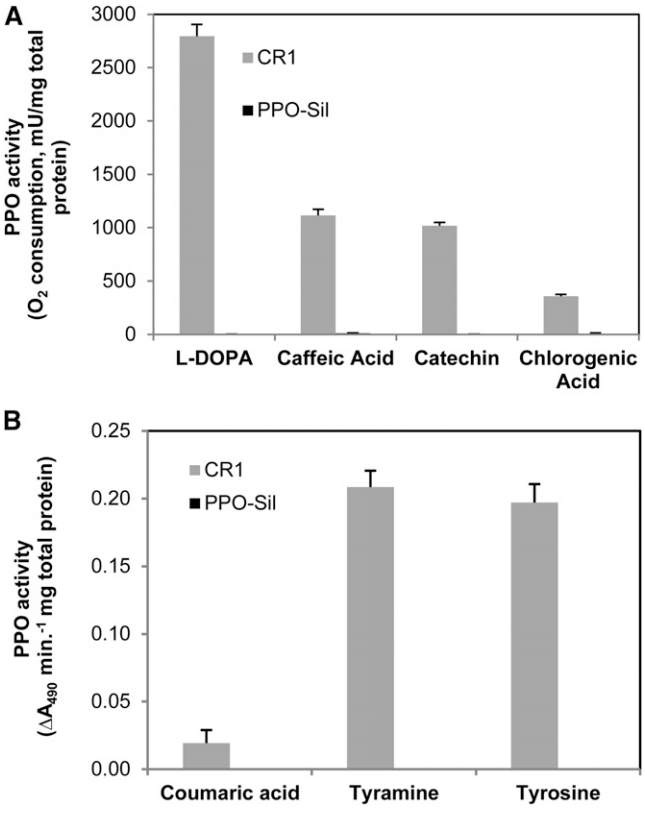

Figure 2. Substrate specificity of JrPPO1. A, Polarimetric PPO activity assay using native *o*-diphenols as substrates. One unit (U) of activity is equivalent to 1 μmol of O_2 consumed per minute (Stewart et al., 2001). B, Spectrophotometric PPO activity assay using native monophenols as substrates. In all experiments, leaf protein extracts from wild-type walnut (CR1) and PPO-silenced walnut lines (PPO-Sil; lines 9-5-1, 5-10-2, and 1-2-15) were assayed. For each sample, the mean PPO activity from two to three replicates (± SEM) is shown.

Transcript and Metabolite Profiling of PPO-Silenced Walnut Lines

To gain a better understanding of how the silencing of *jrPPO1* leads to cell death, we performed global transcript profiling and global metabolite profiling of leaves collected from matched wild-type and PPO-silenced

Table I. *JrPPO1 substrate kinetics*

One milliunit (mU) is equivalent to 1 nmol of oxygen (O_2) consumed per minute.

Substrate	K_m	V_{max}	Catalytic Efficiency (V_{max}/K_m)
	mM	*mU mg^{-1} total protein*	
L-DOPA	17.0	10,000	590
Catechin	3.0	1,667	550
Chlorogenic acid	1.1	455	433
Caffeic acid	7.0	2,500	358

walnut plants. Multiple leaf tissue samples were collected from four separate wild-type trees (comparable to Fig. 3A) and from four separate PPO-silenced trees (comparable to Fig. 3B). RNA sequencing (RNA-seq) was performed on RNA isolated from three wild-type leaf samples and three PPO-silenced leaf samples using an Illumina HiSeq2000. Metabolite profiling was performed on 16 wild-type metabolite extracts and 16 PPO-silenced metabolite extracts using both liquid chromatography-mass spectroscopy and gas chromatography-mass spectroscopy.

Because the walnut genome has not yet been sequenced, reads from RNA-seq analysis were aligned to a previously assembled and annotated walnut transcriptome database containing 85,045 contigs (You et al., 2012). Substantial expression (≥20 aligning reads) was detected for 53,994 of these contigs in our data set. Multidimensional scaling of log-transformed count data using edgeR (Robinson et al., 2010) demonstrated clustering of the three wild-type replicates and clustering of the three PPO-silenced replicates (Supplemental Fig. S6). As expected, sequence reads aligning to the *neomycin phosphotransferase II* gene (the plant-selectable marker gene on the RNAi construct) were abundant in the PPO-silenced samples (3,363 total reads) and essentially absent in the wild-type samples (two total reads; presumably misalignments). In total, 93 contigs in the walnut transcriptome database showed statistically significant differential expression between the PPO-silenced lines and the wild-type controls (Supplemental Table S1). BLASTX analysis against The Arabidopsis Information Resource 10 Proteins database was performed to identify putative Arabidopsis homologs of the differentially expressed walnut genes. The Arabidopsis Genome Initiative numbers of these putative homologs (Supplemental Table S1) were then analyzed using BioMaps software, which identifies and statistically analyzes overrepresented functional categories in global data sets (Katari et al., 2010). This analysis revealed overrepresentation of cell wall-associated genes (P = 0.001), all of which were expressed at higher levels in the PPO-silenced lines (Supplemental Table S2). Visual inspection of the data also revealed that many of the overexpressed genes in PPO-silenced lines had predicted functions in the metabolism of phenolic compounds, especially the phenylpropanoid pathway, including putative cinnamic acid 4-hydroxylase, 4-coumarate-CoA ligase, hydroxycinnamoyl-CoA shikimate/quinate hydroxycinnamoyl transferase, and 4-coumaroylester 3′-hydroxylase genes (Fig. 4).

Metabolite profiling revealed a total of 83 small molecules showing statistically significant differences in abundance between wild-type and PPO-silenced leaf samples (Supplemental Table S3). Strikingly, out of the 10 metabolites that showed the most significant differences in abundance between wild-type and PPO-silenced lines (i.e. lowest associated P values), seven are phenolic compounds or derivatives of phenolic compounds. Large increases in many metabolites derived from the phenylpropanoid pathway were observed in the PPO-silenced lines, most notably flavonoids such as catechin, gallocatechin, and eriodictyol (Fig. 4). The phenylpropanoid pathway also produces the precursors to lignin, including sinapic acid and ferulic acid, which were elevated 3.6- and 1.6-fold, respectively, in the PPO-silenced lines. However, subsequent analyses of H lignin, S lignin, G lignin, and total lignin content in wild-type and PPO-silenced walnut leaves revealed no significant alterations in lignin composition (Supplemental Fig. S7). Regardless, both RNA-seq data and metabolite data suggest an increased activity of the phenylpropanoid pathway in PPO-silenced walnut plants.

In addition to Phe (the starting point of the phenylpropanoid pathway), metabolism involving the other aromatic amino acids was also altered in the PPO-silenced walnut lines. For example, the Trp derivatives tryptamine and serotonin displayed large increases in abundance in the PPO-silenced lines (6.1- and 8.6-fold,

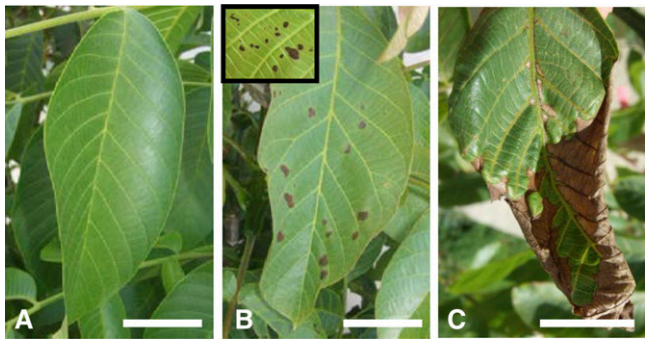

Figure 3. Silencing of *jrppo1* induces a lesion mimic phenotype. A, Wild-type walnut leaf. B, PPO-silenced line, early season (June). Inset, magnified view of necrotic lesions from abaxial side of leaf. C, PPO-silenced line, late season (September). The development of the necrotic lesions was not associated with the presence of any detectable pathogen. Bars = 4 cm.

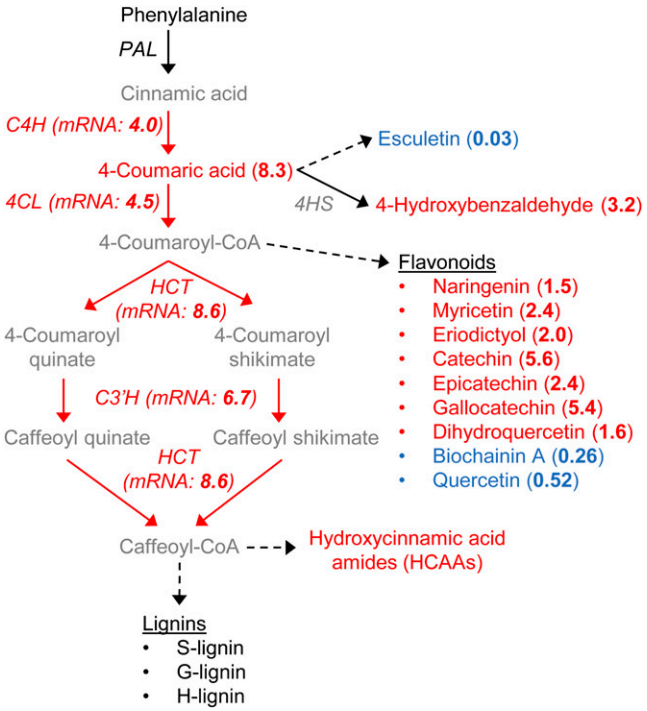

Figure 4. Silencing of *jrPPO1* alters activity of the phenylpropanoid pathway in walnut. Metabolites are colored to represent changes in abundance in the PPO-silenced plant lines relative to the wild type: red indicates increased abundance, blue indicates decreased abundance, black indicates no change, and gray indicates not detected. Quantitative values representing fold change (PPO-silenced lines/wild type) are denoted in bold. The same color scheme is used to depict enzymes, with corresponding mRNA abundance ratios (PPO silenced/wild type) denoted in bold. Dashed arrows represent multiple enzyme-catalyzed reactions. PAL, Phe ammonia lyase; C4H, cinnamic acid 4-hydroxylase (walnut contigs 25466, 65385); 4HS, 4-hydroxybenzaldehyde synthase; 4CL, 4-coumarate-CoA ligase (walnut contig 19023); HCT, hydroxycinnamoyl-CoA shikimate/quinate hydroxycinnamoyl transferase (walnut contigs 12875, 58137, 17482); C3′H, 4-coumaroylester 3′-hydroxylase (walnut contigs 81814, 06713, 81815, 68910, 06709).

respectively). The most striking alterations, however, were observed in the metabolism of Tyr. As summarized in Figure 5, three major pathways of Tyr metabolism are the tyramine pathway, the L-DOPA pathway, and the 4-hydroxyphenylpyruvate pathway (Zhang et al., 2005; Maeda and Dudareva, 2012). PPO-silenced plants displayed a massive increase in tyramine levels (9.3-fold), suggesting increased activity of this pathway. 4-hydroxyphenylpyruvate was not detected in our metabolite extracts, but its derivatives α-tocopherol, β-tocopherol, δ-tocopherol, and γ-tocopherol were all significantly elevated in PPO-silenced plants, suggesting increased activity of the 4-hydroxyphenylpyruvate pathway (Riewe et al., 2012). By contrast, the L-DOPA pathway, whose initial step involves the *o*-hydroxylation of Tyr by an as-yet uncharacterized enzyme (Lee and Facchini, 2011), appears to be essentially inactive in the PPO-silenced lines. Although L-DOPA itself was not detected, the levels of the L-DOPA derivative 5,6-dihydroxyindole were decreased more than 95% in the PPO-silenced lines. Dopamine can be synthesized via either by the L-DOPA pathway or by the tyramine pathway through successive *o*-hydroxylation and decarboxylation of Tyr (the order of reactions depends on the pathway; Fig. 5). Dopamine levels were also dramatically reduced in PPO-silenced lines (>80% reduction). The simplest interpretation of these findings is that the *o*-hydroxylation of Tyr and tyramine is blocked in the PPO-silenced lines, leading to the accumulation of tyramine and the shunting of Tyr metabolism into alternative metabolic pathways, such as 4-hydroxyphenylpyruvate pathway (Fig. 5).

The accumulation of aromatic amines such as tyramine, tryptamine, and serotonin is often associated with the synthesis of hydroxycinnamic acid amides (HCAAs), which are deposited into the cell wall, increasing its strength and reducing its digestibility (Jang et al., 2004; Ishihara et al., 2008). HCAAs are produced through the condensation of aromatic amines and hydroxycinnamoyl-CoA thioesters, often in response to wounding or pathogen challenge (Guillet and De Luca, 2005; Muroi et al., 2009). Because both aromatic amines and phenylpropanoid-derived hydroxycinnamoyl-CoA thioesters are presumably elevated in PPO-silenced lines, we examined HCAA accumulation in situ by staining walnut leaf sections with Neu's reagent and visualizing HCAA fluorescence (Alemanno et al., 2003). Both wild-type and PPO-silenced lines showed clear staining in leaf vasculature, but the PPO-silenced lines also displayed strong HCAA accumulation in the living cells surrounding necrotic lesions (Fig. 6). Thus, it appears that the lesion mimic phenotype in PPO-silenced walnut leaves is associated with the localized accumulation of HCAAs.

The Relationship between PPO and Cell Death

Other than the recent demonstration that the tomato *PPO B* gene is strongly expressed in some tissues undergoing apoptosis (Newman et al., 2011), little previous evidence has linked PPO to programmed cell death. By contrast, several studies have previously implicated aromatic amines in the regulation of cell death and/or lesion mimic phenotypes (in addition to their role in HCAA production). Namely, elevating plant tyramine or serotonin levels by exogenous application or through transgenic approaches can lead to cell death, growth inhibition, and/or lesion mimic phenotypes (Negrel et al., 1993; Ueno et al., 2003; Kang et al., 2007; Fujiwara et al., 2010; Kim et al., 2011). Given that *jrPPO1*-silenced lines display a lesion mimic phenotype and have highly elevated tyramine and serotonin levels (approximately 9-fold increases in each relative to the wild type), we were curious whether exogenous treatment with tyramine or serotonin could induce de novo lesion formation in wild-type walnut leaves. Thus, the petioles of detached wild-type walnut leaves were incubated in solutions of 5 mM tyramine or 5 mM serotonin, mimicking the transpirational uptake system and aromatic amine concentrations

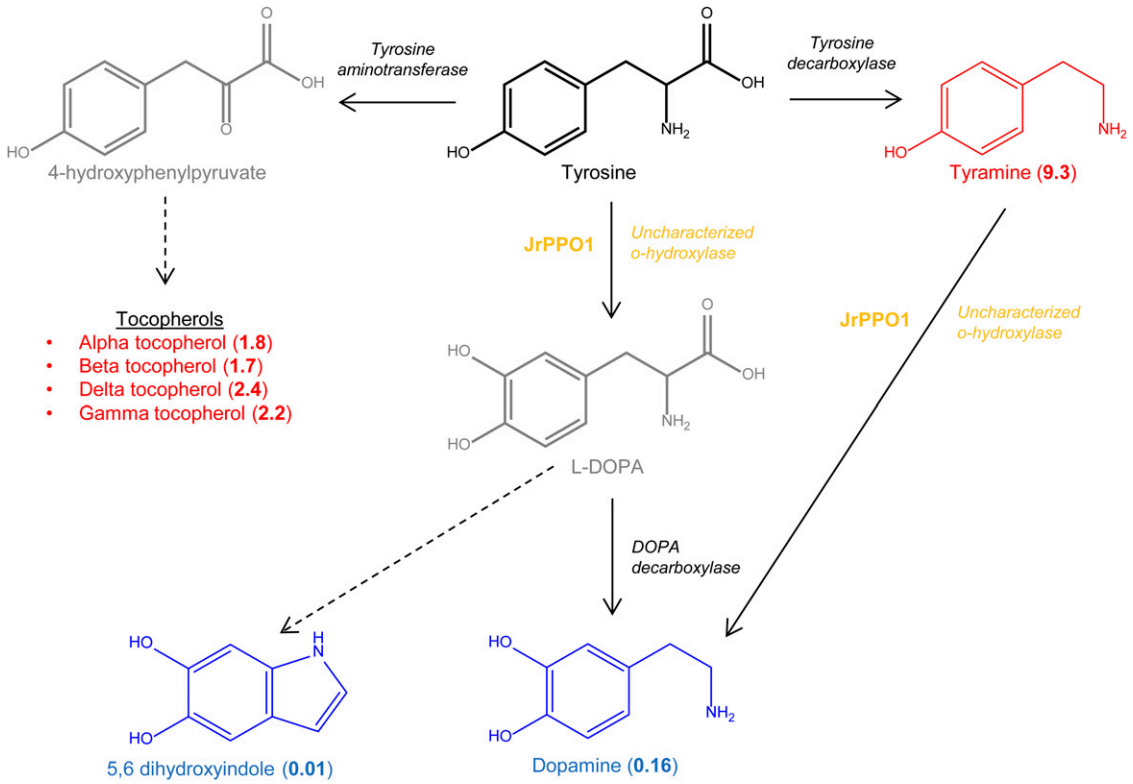

Figure 5. Silencing of *jrPPO1* has direct effects on Tyr metabolism in walnut. Metabolites are colored to represent changes in abundance in the PPO-silenced plant lines relative to the wild type: red indicates increased abundance, blue indicates decreased abundance, black indicates no change, and gray indicates not detected. Quantitative values representing fold change (PPO-silenced lines/wild type) are denoted in bold. Dashed arrows represent multiple enzyme-catalyzed reactions. Proposed reactions catalyzed by JrPPO1 are denoted in orange.

previously utilized by Ueno et al. (2003) in their investigations of the Sekiguchi lesion mutant of rice. Relative to detached leaves incubated in water, serotonin treatment typically caused a darkening of the walnut leaf midrib after 2 to 4 d (data not shown), potentially due to oxidation of serotonin by native peroxidases (Ishihara et al., 2008). By contrast, incubation with tyramine typically caused the spontaneous development of expanding necrotic lesions in the leaf lamina after 2 to 4 d, often in close association with leaf veins (Fig. 7). Thus, exposure of wild-type leaves to elevated levels of tyramine results in a near phenocopy of the lesion mimic phenotype observed in PPO-silenced lines.

DISCUSSION AND CONCLUSION

Although Vaughn et al. (1988) suggested that PPOs are not involved in the metabolism of phenolic compounds in healthy, intact cells, several more recent studies have demonstrated that some PPOs do serve as biosynthetic enzymes required for the production of specialized phenolic-derived pigments (aurones, betalins) and other secondary metabolites (Joy et al., 1995; Cho et al., 2003; Gandía-Herrero et al., 2005). Using a reverse genetics approach, we attempted to overexpress and silence the single PPO gene in walnut, *jrPPO1*, to determine its physiological function. Interestingly, we were unable to recover any *jrPPO1* overexpressing lines, while silencing of *jrPPO1* was very efficient (Fig. 1). Although PPOs have been overexpressed in a variety of other plant species, it is possible that successful overexpression of PPO in walnut leads to a lethal phenotype. Alternatively, given the very high basal level of JrPPO1 activity in walnut (Escobar et al., 2008), it is possible that attempts to express this gene at an even higher level simply result in cosuppression, as was observed in lines 40-1-1 and 78-2-8. In any case, further analysis was restricted to *jrPPO1*-silenced lines, all of which demonstrated more than 95% reduction in leaf PPO activity.

Several studies have shown that PPOs are quite recalcitrant to high-level recombinant protein production in nonplant systems (Sullivan et al., 2004; Wu et al., 2010; Richter et al., 2012). Thus, we decided to analyze the catalytic activity of JrPPO1 directly in crude leaf protein extracts, using the PPO-silenced lines as controls. Regardless of the type of PPO enzyme activity assay (polarimetric, spectrophotometric) or the substrate (monophenol, *o*-diphenol), PPO-silenced lines displayed essentially no activity, indicating that measured activity in wild-type protein extracts could be

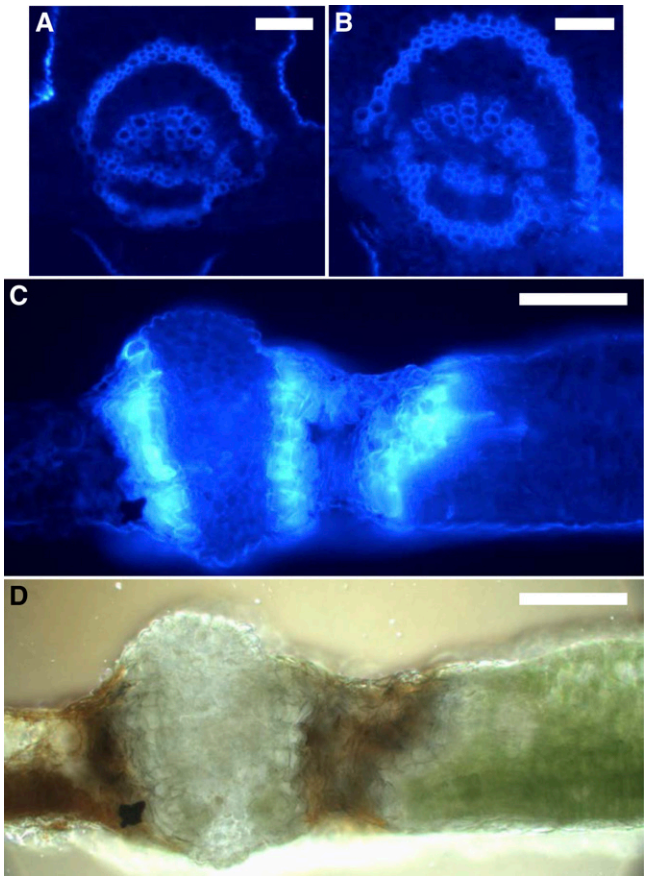

Figure 6. Staining HCAAs in walnut leaf sections. A, Wild-type walnut leaf showing HCAA staining (blue-white fluorescence) in the vasculature. B, Leaf from a PPO-silenced line displaying pattern of HCAA staining similar to the wild type. C, HCAA staining in a region of a PPO-silenced leaf displaying lesion development. D, Light micrograph of the leaf section shown in C. The brown areas are necrotic lesions. All fluorescence micrographs were taken with identical illumination conditions. Bars = 100 μm.

attributed to JrPPO1. Catecholase activity was measured by monitoring the rate of oxygen consumption using a Clark oxygen electrode (polarimetric assay), and calculated kinetic parameters using native *o*-diphenols as substrates (Table I) were comparable to previously reported values in other plant species (Mesquita and Queiroz, 2013). Unlike many plant PPOs, JrPPO1 also displays tyrosinase activity and was capable of oxidizing all tested native monophenols. The rate of in vitro monophenol oxidation was only about 2% of the rate of *o*-diphenol oxidation (Supplemental Fig. S2), but this is comparable to characterized tyrosinase:catecholase activity ratios in apple (*Malus domestica*) and potato, two of the best-characterized plant tyrosinases (Selinheimo et al., 2007). Thus, JrPPO1 has the capability to oxidize a wide variety of native phenolic compounds in vitro, though this does not provide direct evidence that these same reactions occur in vivo.

Once PPO-silenced walnut plants were transferred from tissue culture to soil, it became apparent that many of the developing leaves displayed abnormal necrotic lesions. These lesions were absent from control plants germinated from the same somatic embryo line Chandler1 (CR1) and from walnut plants derived from CR1 embryos transformed with other RNAi constructs (Escobar et al., 2002). Based on extensive pathogen testing, we have concluded that these lesions are not associated with disease. Similar lesion mimic phenotypes have been observed in a variety of transgenic plants in which antioxidant levels (Takahashi et al., 1997), carbohydrate metabolism (Mittler and Rizhsky, 2000), defense-associated genes (Shirano et al., 2002), or phenolic metabolism (Di Fiore et al., 2002) have been manipulated. The absence of elevated reactive oxygen species levels, SA, and oxidative damage in PPO-silenced lines points to a subtle, potentially metabolic, connection between cell death and PPO in walnut.

Lacking any obvious mechanistic connections between the observed lesion mimic phenotype and PPO, we decided to carry out comparative transcriptomics and metabolomics studies on PPO-silenced and wild-type walnut leaves. Substantial alterations in both the transcriptome and the metabolome were observed, but the inherent challenge of this approach is separating the direct effects of silencing *jrPPO1* from the nonspecific, indirect responses triggered by cell death and the lesion mimic phenotype. Thus, data analysis was focused on the following questions. (1) Which of the observed changes are caused directly by the absence of PPO? (2) Which of these direct effects is tied to the activation of cell death? (3) Which of the observed changes are simply general responses to the damage caused by the activation of cell death in PPO-silenced lines? In an attempt to answer the first of these questions, we focused our initial

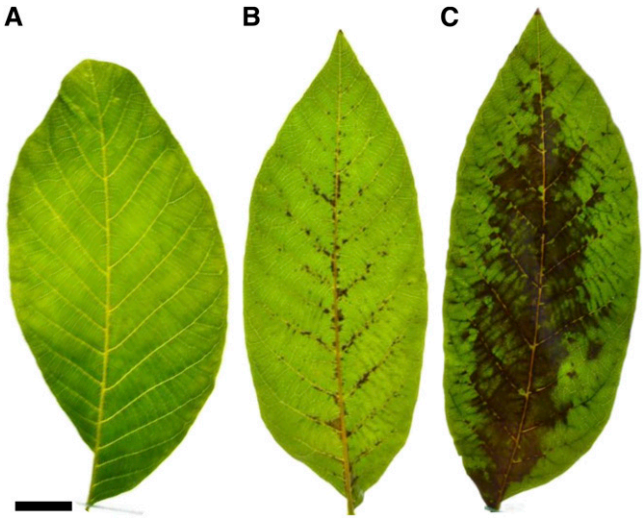

Figure 7. Treatment of wild-type walnut leaves with exogenous tyramine leads to the development of necrotic lesions. A, Detached wild-type leaf incubated in water for 4 d. B, Detached wild-type leaf incubated in a 5 mM solution of tyramine for 2 d. C, Detached wild-type leaf incubated in a 5 mM solution of tyramine for 4 d. Bars = 2 cm.

data analysis on the phenolic compounds native to walnut that can serve as substrates for JrPPO1 in vitro (Fig. 2).

Assuming that JrPPO1 actively oxidizes a phenolic compound in vivo, the most naive model would posit that plants lacking PPO would accumulate its phenolic substrate(s) with a corresponding decrease in the reaction products. Levels of the *o*-diphenols caffeic acid and cryptochlorogenic acid (an isomer of chlorogenic acid, which was not detected) were not significantly altered in the PPO-silenced lines, so these compounds were not further investigated. By contrast, the *o*-diphenol catechin was substantially increased in PPO-silenced lines. However, this increase occurred in concert with elevated levels of many other flavonoids (most of which are not feasible substrates for PPO) and an apparent upregulation of the phenylpropanoid pathway as a whole (Fig. 4). Thus, increases in catechin are more likely attributable to a general increase in phenylpropanoid metabolism than to a specific role as an in vivo substrate for JrPPO1. Similarly, elevated levels of *p*-coumaric acid are likely attributable to a generalized increase in the activity of the phenylpropanoid pathway, including induction of a cinnamic acid 4-hydroxylase gene, which encodes the enzyme responsible for the synthesis of *p*-coumaric acid (Fig. 4). Thus, none of the aforementioned phenolic compounds are likely to be direct targets of JrPPO1 activity in vivo.

By contrast, the effects of PPO silencing on the metabolism of Tyr do point to a direct role for JrPPO1 in phenolic metabolism in walnut. To be clear, Tyr levels (and the levels of Phe and Trp) were unaltered in PPO-silenced lines, as might be expected considering the complex feedback mechanisms that maintain aromatic amino acid homeostasis (Tzin and Galili, 2010). However, PPO-silenced lines displayed dramatic alterations in all three major pathways of Tyr catabolism, with increases in metabolites derived from the 4-hydroxyphenylpyruvate pathway (tocopherols), elevated tyramine levels, and decreased levels of L-DOPA-derived 5,6-dihydroxyindole and dopamine (Fig. 5). Quantitatively, these are among the largest changes observed in the metabolite profiling data, with tyramine among the five metabolites showing the largest increases in PPO-silenced lines (9.3-fold) and dopamine and 5,6-dihydroxyindole among the five metabolites showing the largest decreases in PPO-silenced lines (0.16- and 0.01-fold, respectively). As summarized in Figure 5, the production of 5,6-dihydroxyindole requires the *o*-hydroxylation of Tyr, and the production of dopamine requires the *o*-hydroxylation of either Tyr or tyramine. The enzymes responsible for these activities have not been characterized in plants (Lee and Facchini, 2011). JrPPO1 has demonstrated these activities in vitro (Fig. 2), and the silencing of JrPPO1 leads to clear increases in substrate (tyramine) or alternative metabolic pathways (4-hydroxyphenylpyruvate pathway) and clear decreases in products (5,6-dihydroxyindole, dopamine). Thus, we propose that JrPPO1 catalyzes the *o*-hydroxylation of Tyr and tyramine in vivo as a fundamental feature of aromatic amino acid metabolism in walnut leaves.

If JrPPO1 catalyzes the *o*-hydroxylation of Tyr and tyramine in intact cells, then the enzyme and its substrates must be located in the same subcellular compartment, at least transiently. Almost all PPOs are chloroplast localized (Steffens et al., 1994), and subcellular localization predictors place JrPPO1 in the chloroplast with high confidence (Predotar: plastid, 0.9; MultiLoc: chloroplast, 0.97; Small et al., 2004; Höglund et al., 2006). Likewise, the major enzymes of Tyr biosynthesis have been localized to the chloroplast (Tzin and Galili, 2010), placing JrPPO1 and Tyr in the same compartment. Tyr decarboxylase, the enzyme that converts Tyr to tyramine, has been localized to the cytosol in Arabidopsis (Lehmann and Pollmann, 2009), so tyramine would presumably need to be transported back to the chloroplast for catalysis by PPO.

The recent characterization of an Arabidopsis Tyr aminotransferase mutant provides an interesting parallel to our findings related to Tyr metabolism (Riewe et al., 2012). Tyr aminotransferase catalyzes the conversion of Tyr to 4-hydroxyphenylpyruvate (Fig. 5). As expected, the Tyr aminotransferase mutant showed decreased flux through the 4-hydroxyphenylpyruvate pathway, as demonstrated by large reductions in tocopherol levels. Tyramine was elevated approximately 2.5-fold in the mutant, demonstrating metabolic counterbalancing of the Tyr catabolic pathways, as was also observed in our PPO-silenced walnut plants. Dopamine was not detected in the samples, which is interesting given that Arabidopsis is one of the few plants that lack PPO genes (Tran et al., 2012).

If JrPPO1 plays a fundamental role in Tyr metabolism in walnut, then a direct product of disrupted Tyr metabolism should presumably be responsible for the observed lesion mimic phenotype in PPO-silenced lines. Previous studies have shown that the exogenous application of tyramine to rice cell cultures or to tobacco (*Nicotiana tabacum*), soybean (*Glycine max*), corn (*Zea mays*), and sunflower (*Helianthus annuus*) callus causes cell death (Christou and Barton, 1989; Negrel et al., 1993). Similarly, overexpression of Tyr decarboxylase in rice leads to massively elevated tyramine levels and stunted growth, sterility, and other toxicity symptoms (Kang et al., 2007). Exogenous application of tyramine to wild-type walnut leaves triggers the development of spontaneous necrotic lesions that are a near phenocopy of the lesion mimic phenotype observed in PPO-silenced lines (Fig. 7). Thus, the hyperaccumulation of the toxic metabolite tyramine may underlie the activation of cell death pathways in PPO-silenced walnut lines.

Many of the other observed changes in the leaf transcriptome and metabolome of PPO-silenced walnut lines may simply be stress responses associated with the activation of cell death and the lesion mimic phenotype. For example, the accumulation of HCAAs is typically associated with wounding, pathogen challenge, or other stressors (Facchini et al., 2002; Guillet and De Luca, 2005). Thus, the observed accumulation of HCAAs around necrotic lesions in the PPO-silenced walnut lines (Fig. 6) is likely a general response to the damage caused

by the lesions, not a direct effect of the absence of JrPPO1. Azelaic acid, a dicarboxylic acid that was recently characterized as a metabolic marker of oxidative membrane damage and cell death (Zoeller et al., 2012), is also highly elevated (22-fold) in PPO-silenced lines (Supplemental Table S3). The phenylpropanoid pathway and its products (e.g. flavonoids) are strongly induced by stress, including wounding and pathogen challenge (Dixon and Paiva, 1995; Dixon et al., 2002; Mikulic-Petkovsek et al., 2011). Likewise, synthesis of the Trp derivatives tryptamine and serotonin is up-regulated by pathogen challenge and in tissues undergoing abscission (Ramakrishna et al., 2011). It is also possible that Phe- and Trp-associated pathways are affected by the disruption of Tyr metabolism in PPO-silenced lines through feedback to the shikimate pathway, which generates the precursors of all aromatic amino acids (Tzin and Galili, 2010). Regardless of the regulatory mechanisms, alterations in HCAAs, azelaic acid, Phe metabolism, and Trp metabolism are most likely secondary effects of the silencing of JrPPO1.

An interesting exception to the general up-regulation of the phenylpropanoid pathway and its derivatives in PPO-silenced lines is the hydroxycoumarin esculetin (Fig. 4). The silencing of *jrPPO1* caused dramatic reductions in esculetin, which was readily quantified in all wild-type walnut leaf samples, but was detectable in only one of the 16 samples derived from PPO-silenced lines (Fig. 4; Supplemental Table S3). Although the metabolism of esculetin is not well understood, proposed biosynthesis pathways start with coumaric acid (Blagbrough et al., 2010), an in vitro substrate of JrPPO1. Further, Sato (1967) previously implicated a chloroplast-localized phenolase (PPO) in the synthesis of esculetin based on in vitro studies using protein extracts from *Saxifraga stolonifera*. Our results provide support for the hypothesis that PPO is directly involved in esculetin biosynthesis in vivo, potentially via the oxidation of caffeic acid (Sato, 1967) or via the hydroxylation of umbelliferone (Garcia-Molina et al., 2013; Supplemental Fig. S8). Esculetin can act as an antioxidant and may contribute to plant defense responses (Blagbrough et al., 2010), but very little is known about its specific functional role(s). It is therefore unclear how the loss of esculetin might alter plant physiology and/or influence the lesion mimic phenotype in *jrPPO1*-silenced walnuts.

Overall, our results implicate JrPPO1 as a central enzyme in the metabolism of Tyr and esculetin in walnut, though further research (e.g. radioactive pulse labeling) will be required to definitively assign its role. It is unclear whether PPO enzymes serve similar functions in other plant species, but several previous studies suggest that our findings are not universal. Expression of an antisense PPO gene in tomato resulted in complete silencing of all members of the PPO gene family, but these PPO-silenced plants were phenotypically normal (Thipyapong et al., 2004). In an earlier study, the treatment of mung bean (*Vigna radiata*) seedlings with the PPO inhibitor tentoxin had no apparent effect on levels of the flavonoid rutin or total soluble hydroxyphenolics (Duke and Vaughn, 1982). As previously mentioned, Arabidopsis lacks PPO entirely (Tran et al., 2012). Thus, PPO may not play an important role in the metabolism of phenolic compounds in these plant species, as it does in walnut. Previous studies that have defined a metabolic role for PPOs in vivo have typically implicated biochemical pathways of limited taxonomic distribution. For example, PPO is involved in the biosynthesis of aurone pigments, but this pathway is primarily associated with the Compositae and Leguminosae (Nakayama et al., 2001). In creosote bush, PPO hydroxylates the phenolic compound larreatricin, a key step in the biosynthesis of a group of 8-8′ lignans with very limited distribution (Cho et al., 2003). The biosynthesis of betalin pigments also involves a PPO, but this pathway is limited to the order Caryophyllales (Gandía-Herrero and García-Carmona, 2013). Both the PPO involved in betalin synthesis and JrPPO1 appear to utilize Tyr as a substrate, but the betalin biosynthesis pathway does not involve the production of dopamine (Gandía-Herrero and García-Carmona, 2013). As discussed above, our data suggests that JrPPO1 is the previously uncharacterized *o*-hydroxylase that is required for the synthesis of dopamine from either Tyr or tyramine (Fig. 5). Dopamine is a central intermediate in the biosynthesis of isoquinoline alkaloids, a diverse and economically important group of secondary metabolites (e.g. berberine, morphine, codeine; Tzin and Galili, 2010). Unfortunately, almost nothing is currently known about the alkaloid composition of walnut, so future studies will be required to define the potential role for PPO in isoquinoline alkaloid biosynthesis, both in walnut and in other plant species that produce these biomedically significant secondary metabolites.

MATERIALS AND METHODS

Plant Transformation and Growth

An *Agrobacterium tumefaciens* binary vector designed to silence *jrPPO1* was constructed by cloning the full-length *jrPPO1* sequence into the pART7 plasmid (Gleave, 1992) in the antisense orientation. The initial 1.2 kb of *jrPPO1* was then cloned directly in front of the antisense sequence, generating two 1.2-kb complementary sequences (the 5′ end of *jrPPO1*) separated by a 0.6-kb spacer (the 3′ end of *jrPPO1*). This self-complementary cassette was then cloned into the binary vector pDU97.1005 (A. Dandekar, unpublished data), generating the *jrPPO1* RNAi vector pDE00.0224. The *jrPPO1* overexpression vector pDE98.0806 has been previously described (Escobar et al., 2008). Both vectors were electroporated into the disarmed *A. tumefaciens* strain C58.C1. *A. tumefaciens*-mediated transformation of the walnut (*Juglans regia*) somatic embryo line CR1 and subsequent regeneration of transgenic plants was performed as previously described (McGranahan et al., 1990). After transfer to soil (pots), plants were placed in a lath house (at the University of California, Davis) or outdoor enclosure (at California State University, San Marcos) under ambient conditions with regular irrigation.

PPO Enzyme Activity Assays

Total protein isolation and quantification from walnut leaves was performed as previously described (Escobar et al., 2008). To compare JrPPO1 activity against different *o*-diphenol substrates, oxygen consumption was measured via polarimetric assay using a Clark oxygen electrode as previously described (Stewart et al., 2001). For typical polarimetric assays, substrate concentrations were set at 8 mM, but decreasing concentrations were utilized for selected substrates to calculate K_m and V_{max} using a Lineweaver-Burk plot. Due to relatively low tyrosinase activity of JrPPO1, activity assays utilizing monophenol substrates were performed spectrophotometrically, as previously described (Escobar et al., 2008). For all assays involving wild-type protein extracts, protein extracts from one or

more *jrPPO1*-silenced lines were utilized as negative controls, as activity measured in the wild type but absent from a PPO-silenced line should be attributable to JrPPO1. In addition, control activity assays were performed in the presence of 2 mM kojic acid, a specific inhibitor of PPO (Constabel and Ryan, 1998).

Real-Time RT-PCR

Total RNA was extracted from the leaves of wild-type and PPO-silenced walnut lines using PureLink Plant RNA Reagent (Ambion) according to the manufacturer's specifications. Isolated RNA was further purified using an RNeasy MinElute Cleanup Kit (Qiagen), and then RNA concentration and quality were determined by spectrophotometric analysis and electrophoretic separation using an Experion Automated Electrophoresis System (Bio-Rad). Complementary DNA was synthesized with a Quantitect Reverse Transcription Kit (Qiagen) using 2-μg aliquots of total RNA. Real-time PCR was performed using an Applied Biosystems 7000 machine with Platinum SYBR Green qPCR SuperMix (Applied Biosystems). The primers PPO1-F (5′-TCGTGTTAAGGTTAAGGACTGC-3′) and PPO1-R (5′-CCTTTTCTTTCTTGCTCCTCGAT-3′) were used for analysis of the *jrPPO1* transcript. Primers for the 18S ribosomal RNA transcript, which was utilized as an internal standard, were as previously described (Huang et al., 2011). Cycle threshold values were used to calculate relative changes in gene expression using the $2^{-\Delta\Delta Ct}$ method (Livak and Schmittgen, 2001).

Physiological Characterization of Transgenic Lines

To measure H_2O_2 levels, leaves were first frozen in liquid nitrogen and crushed using a mortar and pestle. Two hundred milligrams of leaf powder were mixed with 1 mL of 5% (w/v) trichloroacetic acid, 50 mg of insoluble poly(vinylpolypyrrolidone) (Sigma), and 50 mg of activated charcoal (Norit SA2, Acros Organics). The slurry was vortexed for 30 s and then centrifuged at 10,000*g* for 10 min and 4°C. The supernatant was diluted 1:10 in 0.25 M sodium phosphate buffer (pH 7.0) and then assayed using an Amplex Red Hydrogen Peroxide/Peroxidase Assay Kit (Invitrogen) as previously described (Shin et al., 2005). As a means to measure lipid peroxidation/general oxidative damage, a thiobarbituric acid reactive substances assay was performed (Umbach et al., 2005). Frozen tissue powder was extracted in 80% (v/v) ethanol (40 mg tissue mL^{-1}), and the thiobarbituric acid reactive substances assay was carried out as described by Umbach et al. (2005).

For lignin analysis, leaves were harvested, flash frozen in liquid nitrogen, and ground with a mortar and pestle. Tissue powder was lyophilized and then sent to the Complex Carbohydrate Research Center (University of Georgia) for analysis by pyrolysis molecular beam mass spectroscopy (Evans and Milne, 1987). Briefly, the lyophilized tissue was pyrolyzed for 2 min at 500°C with helium as the carrier gas and an interface temperature of 350°C. The residues were analyzed using a custom-built Super Sonic Molecular Beam Mass Spectrometer (Extrel model MAX–1000). Biomass standards from eastern cottonwood (*Populus deltoides*; National Institute of Standards and Technology 8492) and Monterey pine (*Pinus radiata*; National Institute of Standards and Technology 8493) were included in all sample runs to check the consistency/performance of the instrument. Because no walnut biomass standard is available, relative values were calculated for total lignin, H lignin, S lignin, and G lignin.

To visualize HCAAs within leaf tissues, fresh hand sections were incubated in Neu's reagent (1% (w/v) 2-amino ethyl diphenyl borinate in absolute methanol) for 5 min and then mounted on a slide in 15% (v/v) glycerol (Gunnaiah et al., 2012). Stained sections were examined using an Olympus IX50 inverted fluorescence microscope under UV illumination with a 4′,6-diamino-phenylindole filter set (350–400 nm excitation wavelength, 420–480 emission wavelength). Using this staining protocol, HCAAs emit a distinct blue-white fluorescence (Alemanno et al., 2003).

Exogenous application of aromatic amines was performed by harvesting fresh leaves and placing the petioles in aqueous solutions of 5 mM serotonin or 5 mM tyramine, essentially as described by Ueno et al. (2003). Control leaves were incubated in water. Walnuts have among the highest native serotonin levels of all plants (up to 300 $\mu g\ g^{-1}$ fresh weight; Feldman et al., 1987). Absolute levels of tyramine have not been measured in walnut, but a recent survey of tyramine in fruits and vegetables found levels ranging from 2 to 220 $\mu g\ g^{-1}$ dry weight (Ly et al., 2008). The aromatic amine solutions were continuously drawn into the leaf through the transpiration stream as the leaves were incubated in a glasshouse for 2 to 4 d. Lesion development was monitored daily.

Pathogen Testing

Walnut blight and walnut anthracnose can cause the development of necrotic lesions on walnut leaves. Thus, we attempted to isolate the causal agents of these diseases (*Xanthomonas arboricola* pv *juglandis* and *Gnomonia leptostyla*, respectively) from the lesions on the leaves of *jrPPO1*-silenced plants. Leaves were surface disinfested by immersion in 15% (v/v) household bleach and 0.1% (v/v) Tween 20 for 1 min followed by three rinses in sterile deionized water. One leaf disc (approximately 20 mm^2) was then punched from the leaf (in tissue around a lesion), and the leaf disc was homogenized in sterile distilled water. Dilutions of the slurry were then plated on Difco nutrient agar for isolation of *X. arboricola* pv *juglandis* (Belisario et al., 1999) or water agar supplemented with 40 mg L^{-1} chloramphenicol and 40 mg L^{-1} streptomycin for isolation of *G. leptostyla* (Belisario et al., 2008). Difco agar plates were incubated at 28°C for 3 d, and water agar plates were incubated at 25°C for 5 d. These experiments were repeated at least three times across multiple growing seasons.

To promote the rapid growth of potential pathogens, detached leaves from PPO-silenced plants were incubated in a moist chamber consisting of a sealed petri plate containing filter paper saturated with sterile water. These plates were placed in a 25°C incubator for 1 week and were monitored daily for lesion expansion, bacterial ooze formation, or the development of acervuli (fruiting bodies). Small black acervuli are diagnostic features of *G. leptostyla* (Cline and Neely, 1983).

Metabolite Profiling

Leaf samples were collected from four wild-type trees and four *jrPPO1*-silenced trees (lines 7-8-1, 173-1-2, 9-5-1, and 9-14). Each leaf sample consisted of three to four mature leaves. The leaf samples (16 wild-type and 16 PPO-silenced) were immediately flash frozen in liquid nitrogen and ground with a mortar and pestle. Frozen tissue powder was lyophilized and sent to Metabolon for untargeted metabolite profiling. Metabolite extraction was performed as previously described (Evans et al., 2009). Metabolite extracts were subjected to three analyses: gas chromatography and mass spectrometry, ultra HPLC and tandem mass spectrometry optimized for basic metabolites, and ultra HPLC and tandem mass spectrometry optimized for acidic metabolites (Cassol et al., 2013). Relative abundance was determined for 194 identified (named) metabolites. Wilcoxon's rank sum tests were used to identify metabolites whose abundance differed significantly between grouped wild-type samples and grouped PPO-silenced samples. *P* values were corrected for multiple hypothesis testing (Benjamini and Hochberg, 1995), and adjusted *P* values ≤ 0.01 were considered statistically significant for the metabolite data set.

RNA-Seq

Leaf samples were collected from three wild-type trees and three *jrPPO1*-silenced trees (lines 7-8-1, 9-5-1, and 9-14). Each leaf sample consisted of three mature leaves and was immediately frozen in liquid nitrogen. RNA isolation and assessment of RNA quality was performed as described above for real-time RT-PCR. Samples utilized for library construction had an RNA Quality Indicator number greater than 8.0. Six sequencing libraries (three independent wild-type biological replicates and three independent PPO-silenced biological replicates) were made using a TruSeq RNA Kit (Illumina) starting with 4 μg of total RNA, according to the manufacturer's specifications. Each sequencing library was barcoded, pooled on a single Illumina flow cell lane, and then sequenced using an Illumina HiSeq 2000 (100-nucleotide paired-end reads) at the University of California, Davis Genome Center.

Demultiplexed sequence reads were trimmed with custom scripts, including Scythe (unpublished, available at https://github.com/ucdavis-bioinformatics/scythe) to remove Illumina adapter contamination and sickle (unpublished, available at https://github.com/ucdavis-bioinformatics/sickle) to trim low-quality bases at the 3′ end of reads. Trimmed reads were aligned to a walnut transcriptome assembly consisting of 85,045 contigs using Burrows-Wheeler Aligner version 0.6.1 (Li and Durbin, 2009). The walnut transcriptome was previously assembled from approximately 1 billion 85-nucleotide RNA-seq reads derived from RNA isolated from 20 different walnut tissue samples (You et al., 2012). The BLAST2GO program (Conesa et al., 2005) was utilized for putative functional annotation of the walnut sequences. BLASTX alignment of the walnut sequences to the Arabidopsis (*Arabidopsis thaliana*) proteome was used to identify putative homologous genes, with an *E* value cutoff of 1e–05. Differential expression analysis of count data were performed using DESeq version 1.6 (Anders and Huber, 2010), with *P* values corrected for multiple hypothesis testing (Benjamini and Hochberg, 1995). Adjusted *P* values ≤ 0.05 were considered statistically significant for the RNA-seq data set. Contigs with less than 20 total counts were excluded from analysis.

Initial analysis of the differentially expressed gene set (Supplemental Table S1) surprisingly revealed that *jrPPO1* was not identified as differentially

expressed. This was because one of the three analyzed RNAi lines showed a relatively high level of *jrPPO1* counts compared with both of the other transgenic lines. (The three wild-type lines had 1,230, 2,545, and 1,252 *jrPPO1* counts, and the three RNAi lines had 301 [line 9-5-1], 549 [line 9-14], and 2,284 [line 7-8-1] counts). Despite this unexpected result, several lines of evidence suggest that the 7-8-1 transgenic line is silenced for *jrPPO1*. First, PPO activity assays performed using the same tissue sample that was subsequently utilized for RNA isolation, and RNA-seq analysis showed less than 5% of wild-type PPO activity in line 7-8-1 (in agreement with previous PPO activity assays performed on this line; Fig. 1). Second, subsequent analyses of six separate RNA samples isolated from 7-8-1 and analyzed by real-time PCR showed dramatically reduced *jrPPO1* transcript levels, mirroring the activity data (Supplemental Fig. S1). Finally, multidimensional scaling analysis of the overall RNA-seq transcriptome profile of 7-8-1 clearly groups this line with the other two PPO-silenced lines, separate from the wild-type samples (Supplemental Fig. S6). Thus, we ultimately decided to retain the RNA-seq data from line 7-8-1 in our final analysis.

To investigate the possibility of off-target effects of RNAi, TBLASTX was used to align the *jrPPO1* gene sequence to the sequences of all identified differentially expressed genes. No significant hits were found, suggesting that the observed changes in gene expression were not associated with the silencing of nontarget genes possessing a high degree of sequence similarity to *jrPPO1*.

Sequence data from this article can be found in the GenBank/EMBL data libraries under accession number SRP036081.

Supplemental Data

The following materials are available in the online version of this article.

Supplemental Figure S1. Real-time RT-PCR analysis of *jrPPO1* transcript levels in wild-type and PPO-silenced leaves.

Supplemental Figure S2. Comparison of tyrosinase and catecholase activities of JrPPO1.

Supplemental Figure S3. SA levels in metabolite extracts from wild-type (CR1) and PPO-silenced walnut leaves.

Supplemental Figure S4. H_2O_2 levels in leaf extracts from wild-type walnut (CR1) and PPO-silenced lines.

Supplemental Figure S5. Malondialdehyde levels in metabolite extracts from wild-type (CR1) and PPO-silenced walnut leaves.

Supplemental Figure S6. Multidimensional scaling plot of log-transformed RNA-seq count data.

Supplemental Figure S7. Lignin analysis of wild-type (CR1) and PPO-silenced walnut lines.

Supplemental Figure S8. Two proposed esculetin biosynthesis pathways involving PPO.

Supplemental Table S1. List of differentially regulated contigs between wild-type and *jrPPO1*-silenced plants.

Supplemental Table S2. BioMaps analysis of genes differentially expressed in PPO-silenced walnut lines.

Supplemental Table S3. Comparison of metabolite levels in wild-type and PPO-silenced walnut leaves.

ACKNOWLEDGMENTS

We thank Richard Bostock (University of California [Davis]) for his advice on pathogen testing and the lesion mimic phenotype, William Kristan (California State University [San Marcos]) for assistance with statistical analyses, Monica Britton and Russell Reagan (University of California [Davis]) for bioinformatics analyses, Gale McGranahan (University of California [Davis]) for plant transformation and tissue culture, and Kurt Patterson (California State University [San Marcos]) for technical assistance.

Received September 16, 2013; accepted January 21, 2014; published January 21, 2014.

LITERATURE CITED

Alemanno L, Ramos T, Gargadenec A, Andary C, Ferriere N (2003) Localization and identification of phenolic compounds in *Theobroma cacao* L. somatic embryogenesis. Ann Bot (Lond) **92:** 613–623

Anders S, Huber W (2010) Differential expression analysis for sequence count data. Genome Biol **11:** R106

Belisario A, Scotton M, Santori A, Onofri S (2008) Variability in the Italian population of *Gnomonia leptostyla*, homothallism and resistance of *Juglans* species to anthracnose. For Pathol **38:** 129–145

Belisario A, Zoina A, Pezza L, Luongo L (1999) Susceptibility of species of *Juglans* to pathovars of *Xanthomonas campestris*. Eur J Forest Pathol **29:** 75–80

Benjamini Y, Hochberg Y (1995) Controlling the false discovery rate: a practical and powerful approach to multiple testing. J R Stat Soc, B **57:** 289–300

Bhonwong A, Stout MJ, Attajarusit J, Tantasawat P (2009) Defensive role of tomato polyphenol oxidases against cotton bollworm (*Helicoverpa armigera*) and beet armyworm (*Spodoptera exigua*). J Chem Ecol **35:** 28–38

Blagbrough IS, Bayoumi SA, Rowan MG, Beeching JR (2010) Cassava: an appraisal of its phytochemistry and its biotechnological prospects. Phytochemistry **71:** 1940–1951

Cassol E, Misra V, Holman A, Kamat A, Morgello S, Gabuzda D (2013) Plasma metabolomics identifies lipid abnormalities linked to markers of inflammation, microbial translocation, and hepatic function in HIV patients receiving protease inhibitors. BMC Infect Dis **13:** 203

Cho MH, Moinuddin SGA, Helms GL, Hishiyama S, Eichinger D, Davin LB, Lewis NG (2003) (+)-Larreatricin hydroxylase, an enantio-specific polyphenol oxidase from the creosote bush (*Larrea tridentata*). Proc Natl Acad Sci USA **100:** 10641–10646

Christou P, Barton KA (1989) Cytokinin antagonist activity of substituted phenethylamines in plant cell culture. Plant Physiol **89:** 564–568

Cline S, Neely D (1983) Penetration and infection of leaves of black walnut by *Marssonina juglandis* and resulting lesion development. Phytopathology **73:** 494–497

Colaric M, Veberic R, Solar A, Hudina M, Stampar F (2005) Phenolic acids, syringaldehyde, and juglone in fruits of different cultivars of *Juglans regia* L. J Agric Food Chem **53:** 6390–6396

Conesa A, Götz S, García-Gómez JM, Terol J, Talón M, Robles M (2005) Blast2GO: a universal tool for annotation, visualization and analysis in functional genomics research. Bioinformatics **21:** 3674–3676

Constabel CP, Ryan CA (1998) A survey of wound- and methyl jasmonate-induced leaf polyphenol oxidase in crop plants. Phytochemistry **47:** 507–511

Di Fiore S, Li Q, Leech MJ, Schuster F, Emans N, Fischer R, Schillberg S (2002) Targeting tryptophan decarboxylase to selected subcellular compartments of tobacco plants affects enzyme stability and in vivo function and leads to a lesion-mimic phenotype. Plant Physiol **129:** 1160–1169

Dixon RA, Achnine L, Kota P, Liu CJ, Reddy MS, Wang L (2002) The phenylpropanoid pathway and plant defence: a genomics perspective. Mol Plant Pathol **3:** 371–390

Dixon RA, Paiva NL (1995) Stress-induced phenylpropanoid metabolism. Plant Cell **7:** 1085–1097

Duke SO, Vaughn KC (1982) Lack of involvement of polyphenol oxidase in ortho-hydroxylation of phenolic compounds in mung bean seedlings. Physiol Plant **54:** 381–385

Escobar MA, Leslie CA, McGranahan GH, Dandekar AM (2002) Silencing crown gall disease in walnut (*Juglans regia* L.). Plant Sci **163:** 591–597

Escobar MA, Shilling A, Higgins P, Uratsu SL, Dandekar AM (2008) Characterization of polyphenol oxidase from walnut. J Am Soc Hortic Sci **133:** 852–858

Evans AM, DeHaven CD, Barrett T, Mitchell M, Milgram E (2009) Integrated, nontargeted ultrahigh performance liquid chromatography/electrospray ionization tandem mass spectrometry platform for the identification and relative quantification of the small-molecule complement of biological systems. Anal Chem **81:** 6656–6667

Evans RJ, Milne TA (1987) Molecular characterization of the pyrolysis of biomass. Energy Fuels **1:** 123–137

Facchini PJ, Hagel J, Zulak KG (2002) Hydroxycinnamic acid amide metabolism: physiology and biochemistry. Can J Bot **80:** 577–589

Feldman JM, Lee EM, Castleberry CA (1987) Catecholamine and serotonin content of foods: effect on urinary excretion of homovanillic and 5-hydroxyindoleacetic acid. J Am Diet Assoc **87:** 1031–1035

Fujiwara T, Maisonneuve S, Isshiki M, Mizutani M, Chen L, Wong HL, Kawasaki T, Shimamoto K (2010) Sekiguchi lesion gene encodes a cytochrome P450 monooxygenase that catalyzes conversion of tryptamine to serotonin in rice. J Biol Chem **285:** 11308–11313

Gandía-Herrero F, Escribano J, García-Carmona F (2005) Betaxanthins as substrates for tyrosinase. An approach to the role of tyrosinase in the biosynthetic pathway of betalains. Plant Physiol **138:** 421–432

Gandía-Herrero F, García-Carmona F (2013) Biosynthesis of betalains: yellow and violet plant pigments. Trends Plant Sci **18:** 334–343

Garcia-Molina MO, Munoz-Munoz JL, Garcia-Molina F, Rodriguez-Lopez JN, Garcia-Canovas F (2013) Study of umbelliferone hydroxylation to esculetin catalyzed by polyphenol oxidase. Biol Pharm Bull **36:** 1140–1145

Gleave AP (1992) A versatile binary vector system with a T-DNA organisational structure conducive to efficient integration of cloned DNA into the plant genome. Plant Mol Biol **20:** 1203–1207

Goldfeder M, Kanteev M, Adir N, Fishman A (2013) Influencing the monophenolase/diphenolase activity ratio in tyrosinase. Biochim Biophys Acta **1834:** 629–633

Guillet G, De Luca V (2005) Wound-inducible biosynthesis of phytoalexin hydroxycinnamic acid amides of tyramine in tryptophan and tyrosine decarboxylase transgenic tobacco lines. Plant Physiol **137:** 692–699

Gunnaiah R, Kushalappa AC, Duggavathi R, Fox S, Somers DJ (2012) Integrated metabolo-proteomic approach to decipher the mechanisms by which wheat QTL (Fhb1) contributes to resistance against *Fusarium graminearum*. PLoS ONE **7:** e40695

Höglund A, Dönnes P, Blum T, Adolph HW, Kohlbacher O (2006) MultiLoc: prediction of protein subcellular localization using N-terminal targeting sequences, sequence motifs and amino acid composition. Bioinformatics **22:** 1158–1165

Huang Z, Surana P, Kihara D, Meilan R, Woeste K (2011) *JnCML-like*, an EF-hand motif-containing gene seasonally upregulated in the transition zone of black walnut (*Juglans nigra* L.). American Journal of Molecular Biology **1:** 140–155

Ishihara A, Hashimoto Y, Tanaka C, Dubouzet JG, Nakao T, Matsuda F, Nishioka T, Miyagawa H, Wakasa K (2008) The tryptophan pathway is involved in the defense responses of rice against pathogenic infection via serotonin production. Plant J **54:** 481–495

Jang SM, Ishihara A, Back K (2004) Production of coumaroylserotonin and feruloylserotonin in transgenic rice expressing pepper hydroxycinnamoyl-coenzyme A:serotonin *N*-(hydroxycinnamoyl)transferase. Plant Physiol **135:** 346–356

Joy RW IV, Sugiyama M, Fukuda H, Komamine A (1995) Cloning and characterization of polyphenol oxidase cDNAs of *Phytolacca americana*. Plant Physiol **107:** 1083–1089

Kang S, Kang K, Lee K, Back K (2007) Characterization of rice tryptophan decarboxylases and their direct involvement in serotonin biosynthesis in transgenic rice. Planta **227:** 263–272

Katari MS, Nowicki SD, Aceituno FF, Nero D, Kelfer J, Thompson LP, Cabello JM, Davidson RS, Goldberg AP, Shasha DE, et al (2010) VirtualPlant: a software platform to support systems biology research. Plant Physiol **152:** 500–515

Kim JY, Seo YS, Kim JE, Sung SK, Song KJ, An G, Kim WT (2001) Two polyphenol oxidases are differentially expressed during vegetative and reproductive development and in response to wounding in the Fuji apple. Plant Sci **161:** 1145–1152

Kim YS, Park S, Kang K, Lee K, Back K (2011) Tyramine accumulation in rice cells caused a dwarf phenotype via reduced cell division. Planta **233:** 251–260

Kowalski SP, Eannetta NT, Hirzel AT, Steffens JC (1992) Purification and characterization of polyphenol oxidase from glandular trichomes of *Solanum berthaultii*. Plant Physiol **100:** 677–684

Lee EJ, Facchini PJ (2011) Tyrosine aminotransferase contributes to benzylisoquinoline alkaloid biosynthesis in opium poppy. Plant Physiol **157:** 1067–1078

Lehmann T, Pollmann S (2009) Gene expression and characterization of a stress-induced tyrosine decarboxylase from *Arabidopsis thaliana*. FEBS Lett **583:** 1895–1900

Li H, Durbin R (2009) Fast and accurate short read alignment with Burrows-Wheeler transform. Bioinformatics **25:** 1754–1760

Li L, Steffens JC (2002) Overexpression of polyphenol oxidase in transgenic tomato plants results in enhanced bacterial disease resistance. Planta **215:** 239–247

Livak KJ, Schmittgen TD (2001) Analysis of relative gene expression data using real-time quantitative PCR and the $2^{-\Delta\Delta C}_{T}$ method. Methods **25:** 402–408

Lorrain S, Vailleau F, Balagué C, Roby D (2003) Lesion mimic mutants: keys for deciphering cell death and defense pathways in plants? Trends Plant Sci **8:** 263–271

Ly D, Kang K, Choi JY, Ishihara A, Back K, Lee SG (2008) HPLC analysis of serotonin, tryptamine, tyramine, and the hydroxycinnamic acid amides of serotonin and tyramine in food vegetables. J Med Food **11:** 385–389

Maeda H, Dudareva N (2012) The shikimate pathway and aromatic amino acid biosynthesis in plants. Annu Rev Plant Biol **63:** 73–105

Mahanil S, Attajarusit J, Stout MJ, Thipyapong P (2008) Overexpression of tomato polyphenol oxidase increases resistance to common cutworm. Plant Sci **174:** 456–466

McGranahan GH, Leslie CA, Uratsu SL, Dandekar AM (1990) Improved efficiency of the walnut somatic embryo gene transfer system. Plant Cell Rep **8:** 512–516

Mesquita VLV, Queiroz C (2013) Enzymatic browning. I*n* NAM Eskin, F Shahidi, eds, Biochemistry of Foods. Academic Press, London, pp 387–418

Mikulic-Petkovsek M, Slatnar A, Veberic R, Solar A (2011) Phenolic response in green walnut husk after infection with bacteria *Xanthomonas arboricola pv. juglandis*. Physiol Mol Plant Pathol **76:** 159–165

Mittler R, Rizhsky L (2000) Transgene-induced lesion mimic. Plant Mol Biol **44:** 335–344

Muroi A, Ishihara A, Tanaka C, Ishizuka A, Takabayashi J, Miyoshi H, Nishioka T (2009) Accumulation of hydroxycinnamic acid amides induced by pathogen infection and identification of agmatine coumaroyltransferase in *Arabidopsis thaliana*. Planta **230:** 517–527

Nakayama T, Sato T, Fukui Y, Yonekura-Sakakibara K, Hayashi H, Tanaka Y, Kusumi T, Nishino T (2001) Specificity analysis and mechanism of aurone synthesis catalyzed by aureusidin synthase, a polyphenol oxidase homolog responsible for flower coloration. FEBS Lett **499:** 107–111

Negrel J, Javelle F, Paynot M (1993) Biochemical basis of resistance of tobacco callus tissue cultures to hydroxyphenylethylamines. Plant Physiol **103:** 329–334

Newman SM, Tantasawat P, Steffens JC (2011) Tomato polyphenol oxidase B is spatially and temporally regulated during development and in response to ethylene. Molecules **16:** 493–517

Ramakrishna A, Giridhar P, Ravishankar GA (2011) Phytoserotonin: a review. Plant Signal Behav **6:** 800–809

Richter C, Dirks ME, Gronover CS, Prüfer D, Moerschbacher BM (2012) Silencing and heterologous expression of ppo-2 indicate a specific function of a single polyphenol oxidase isoform in resistance of dandelion (*Taraxacum officinale*) against *Pseudomonas syringae* pv. *tomato*. Mol Plant Microbe Interact **25:** 200–210

Riewe D, Koohi M, Lisec J, Pfeiffer M, Lippmann R, Schmeichel J, Willmitzer L, Altmann T (2012) A tyrosine aminotransferase involved in tocopherol synthesis in Arabidopsis. Plant J **71:** 850–859

Robinson MD, McCarthy DJ, Smyth GK (2010) edgeR: a Bioconductor package for differential expression analysis of digital gene expression data. Bioinformatics **26:** 139–140

Sato M (1967) Metabolism of phenolic substances by the chloroplasts.— III. Phenolase as an enzyme concerning the formation of esculetin. Phytochemistry **6:** 1363–1373

Selinheimo E, NiEidhin D, Steffensen C, Nielsen J, Lomascolo A, Halaouli S, Record E, O'Beirne D, Buchert J, Kruus K (2007) Comparison of the characteristics of fungal and plant tyrosinases. J Biotechnol **130:** 471–480

Shin R, Berg RH, Schachtman DP (2005) Reactive oxygen species and root hairs in *Arabidopsis* root response to nitrogen, phosphorus and potassium deficiency. Plant Cell Physiol **46:** 1350–1357

Shirano Y, Kachroo P, Shah J, Klessig DF (2002) A gain-of-function mutation in an *Arabidopsis* Toll Interleukin1 receptor-nucleotide binding site-leucine-rich repeat type R gene triggers defense responses and results in enhanced disease resistance. Plant Cell **14:** 3149–3162

Small I, Peeters N, Legeai F, Lurin C (2004) Predotar: a tool for rapidly screening proteomes for N-terminal targeting sequences. Proteomics **4:** 1581–1590

Solar A, Colaric M, Usenik V, Stampar F (2006) Seasonal variations of selected flavonoids, phenolic acids and quinones in annual shoots of common walnut (*Juglans regia* L.). Plant Sci **170:** 453–461

Steffens JC, Harel E, Hunt MD (1994) Polyphenol oxidase. *In* BE Ellis, ed, Genetic Engineering of Plant Secondary Metabolism. Plenum Press, New York, pp 275–312

Stewart RJ, Sawyer BJB, Bucheli CS, Robinson SP (2001) Polyphenol oxidase is induced by chilling and wounding in pineapple. Aust J Plant Physiol **28:** 181–191

Sullivan ML, Hatfield RD, Thoma SL, Samac DA (2004) Cloning and characterization of red clover polyphenol oxidase cDNAs and expression of active protein in *Escherichia coli* and transgenic alfalfa. Plant Physiol **136:** 3234–3244

Takahashi H, Chen Z, Du H, Liu Y, Klessig DF (1997) Development of necrosis and activation of disease resistance in transgenic tobacco plants with severely reduced catalase levels. Plant J **11:** 993–1005

Thipyapong P, Hunt MD, Steffens JC (2004) Antisense downregulation of polyphenol oxidase results in enhanced disease susceptibility. Planta **220:** 105–117

Thipyapong P, Steffens JC (1997) Tomato polyphenol oxidase (differential response of the polyphenol oxidase F promoter to injuries and wound signals). Plant Physiol **115:** 409–418

Thygesen PW, Dry IB, Robinson SP (1995) Polyphenol oxidase in potato: a multigene family that exhibits differential expression patterns. Plant Physiol **109:** 525–531

Tran LT, Taylor JS, Constabel CP (2012) The polyphenol oxidase gene family in land plants: lineage-specific duplication and expansion. BMC Genomics **13:** 395

Tzin V, Galili G (2010) New insights into the shikimate and aromatic amino acids biosynthesis pathways in plants. Mol Plant **3:** 956–972

Ueno M, Shibata H, Kihara J, Honda Y, Arase S (2003) Increased tryptophan decarboxylase and monoamine oxidase activities induce Sekiguchi lesion formation in rice infected with *Magnaporthe grisea*. Plant J **36:** 215–228

Umbach AL, Fiorani F, Siedow JN (2005) Characterization of transformed Arabidopsis with altered alternative oxidase levels and analysis of effects on reactive oxygen species in tissue. Plant Physiol **139:** 1806–1820

Vaughn KC, Lax AR, Duke SO (1988) Polyphenol oxidase: the chloroplast oxidase with no established function. Physiol Plant **72:** 659–665

Wang JH, Constabel CP (2004) Polyphenol oxidase overexpression in transgenic *Populus* enhances resistance to herbivory by forest tent caterpillar (*Malacosoma disstria*). Planta **220:** 87–96

Wu YL, Pan LP, Yu SL, Li HH (2010) Cloning, microbial expression and structure-activity relationship of polyphenol oxidases from *Camellia sinensis*. J Biotechnol **145:** 66–72

You FM, Deal KR, Wang J, Britton MT, Fass JN, Lin D, Dandekar AM, Leslie CA, Aradhya M, Luo MC, et al (2012) Genome-wide SNP discovery in walnut with an AGSNP pipeline updated for SNP discovery in allogamous organisms. BMC Genomics **13:** 354

Zhang P, Foerster H, Tissier CP, Mueller L, Paley S, Karp PD, Rhee SY (2005) MetaCyc and AraCyc: metabolic pathway databases for plant research. Plant Physiol **138:** 27–37

Zoeller M, Stingl N, Krischke M, Fekete A, Waller F, Berger S, Mueller MJ (2012) Lipid profiling of the Arabidopsis hypersensitive response reveals specific lipid peroxidation and fragmentation processes: biogenesis of pimelic and azelaic acid. Plant Physiol **160:** 365–378